

Development of Novel Methods to Investigate the Brain at Rest

Desenvolvimento de Novos Métodos para Investigação do Cérebro durante o Estado de Repouso

Sergio Luiz Novi Junior¹, Wagner Alan Aparecido da Rocha, Alex de Castro Carvalho, Giovanni Hering Scavariello, Rodrigo Menezes Forti, Andres Fabian Guiroga Soto, Vinicius Romera Oliveira, Clarissa Lin Yasuda, Rickson Coelho Mesquita

¹Universidade Estadual de Campinas, Campinas, Brasil

Resumo

O funcionamento cerebral parece ser altamente organizado mesmo na ausência de tarefas específicas. Neste trabalho usamos teoria de grafos num experimento de neuroimagem multimodal com ressonância magnética funcional e espectroscopia no infravermelho próximo para entender melhor a conectividade funcional durante o estado de repouso. Nossos resultados sugerem que, independentemente das diferenças entre voluntários, suas propriedades de grafos é muito similar. Além disso, propomos uma nova abordagem para analisar a conectividade de um grupo baseado na frequência de distribuição de links.

Palavras-chave: neuroimagem; conectividade funcional; NIRS; fMRI; teoria de grafos.

Abstract

Brain function appears to be highly organized even in the absence of specific tasks. In this work we use graph theory in a multimodal neuroimaging experiment employing functional magnetic resonance imaging and near-infrared spectroscopy to better understand functional connectivity during the resting state. Our results suggest that, despite differences across subjects, their graph properties are very similar. In addition, we propose a novel approach to analyze group connectivity based on frequency distribution of the links.

Keywords: neuroimaging; functional connectivity; NIRS; fMRI; graph theory.

1. Introduction

The ability to probe brain function noninvasively opened new directions in neuroscience in the early 1990s. With temporal acquisition of sequential images of magnetic resonance imaging at 0.5 Hz, it became possible to infer cortical regions statistically associated with the performance of a given task, such as finger tapping or visual stimulation¹. This approach, known as functional magnetic resonance imaging (fMRI), has become standard in functional neuroscience to understand brain function due to an external task. The blood-oxygen level dependent (BOLD) signal, the most common fMRI measurement, explores changes in the local magnetic field due to variations of deoxy-hemoglobin concentration (Hb) in blood vessels. Compared to baseline, Hb varies during a task due to neurovascular coupling².

In parallel with the advances in fMRI other emerging neuroimaging techniques appeared. One alternative approach to probe brain function is near-infrared spectroscopy (NIRS)^{3,4}. Briefly, NIRS employs near-infrared light (~700 – 900 nm) to measure hemoglobin concentration changes in the brain noninvasively and with temporal resolution of up to 50 Hz. Over the years NIRS has also been shown to be able to probe brain function due to external tasks⁵.

However, even in the absence of a specific task, the brain takes up to 20% of the energy consumed by the body⁶. For a system to demand so much energy at rest, it must be highly organized. Indeed, several studies with fMRI and/or NIRS have reported the presence of functional networks during the resting state (i.e., in the absence of a specific brain function)⁷⁻¹⁰. These studies rely on the comparison of low-frequency (< 0.1 Hz) spontaneous fluctuations of the neuroimaging signal across different regions of the brain. Interestingly, recent studies have suggested that neuropsychiatric disorders, as well as aging, deteriorate reliable features commonly seen in healthy brains¹¹⁻¹⁴.

In resting state functional connectivity, networks are found by correlating the signal from all regions of the brain with a specific region chosen *a priori*. Although this approach has allowed progress about our understanding of the brain, it is very limited since it does not take into account the overall spatial-temporal variations of the brain. A more complete picture of brain function during the resting state can be achieved by using graph theory⁸.

In this work we explore our recent advances in applying graph theory approaches to understand the NIRS and BOLD-fMRI signals of the human brain during the resting state. In particular, we

present a novel perspective to analyze functional connectivity data based on the frequency maps, which aims to answer the question of what connections are common across a group of subjects.

2. Materials and Methods

2.1. Subjects and Experimental Protocol

Twenty healthy subjects (3 female) with age between 18 to 28 years old were recruited for this study. All subjects provided their informed consent previous to data acquisition. The Ethical Committee at the University of Campinas approved the study protocol.

Subjects were laid down inside the MRI and required to perform 5-min baseline runs from 3 to 6 times, totalizing 101 runs. For each run, subjects were instructed to close their eyes and not focus attention in any specific task.

2.2. Data acquisition and pre-processing

We simultaneously acquired data with fMRI and NIRS. The fMRI protocol was performed in a 3T MRI instrument (Philips Achieva), and included structural and functional images. The structural images were T1-weighted with $1 \times 1 \times 1$ mm³ resolution (TE = 3.2 s, TR = 7 ms, TI = 900 ms, 8° flip angle). The functional images were T2*-weighted gradient echo EPI sequences with $3 \times 3 \times 3$ mm³ spatial resolution (TE = 30 ms, TR = 2 s, 90° flip angle).

The NIRS measurement employed a commercial instrument (NIRScout, NIRx Medical Systems) with 32 detectors and 16 sources with 2 wavelengths each (760 and 850 nm). The optical probe contained 64 source-detector combinations (channels) that covered the whole head, including frontal, temporal, parietal and occipital lobes. Prior to acquisition, the channels were digitized with a magnetic digitizer (Polhemus, Fastrak) for later superposition with MRI structural images. The NIRS temporal resolution was 7.8 Hz.

After acquisition, the BOLD signal from fMRI was preprocessed using standard methods from the literature¹⁵. Briefly, we employed slice-timing correction and used data from movement, white matter and cerebrospinal fluid as regressors. Then, the fMRI images were parceled onto 90 regions of interest (ROIs) using a standard anatomical atlas¹⁶. We applied removal of motion artifacts to remove spurious correlations due to motion¹⁵. We corrected motion artifacts with MatLab homemade scripts, while the other preprocessing steps were performed with the UF2C toolbox¹⁷.

Light intensities from each channel in the NIRS data were converted to oxy- (HbO₂), and deoxy-hemoglobin (Hb) concentration changes with the modified Beer-Lambert law¹⁸. Total-hemoglobin concentration (HbT) was obtained by summing HbO₂ and Hb. Channels with low signal-to-noise ratio (SNR < 8) were also discarded from analysis. In practice, the SNR quality check led to an average (standard deviation) loss of 13 (8)

channels. Motion artifacts were visually inspected and manually removed from the data, and the global signal regression was removed with a Principal Component Analysis (PCA) filter¹⁹. All NIRS processing steps were performed on MatLab homemade scripts based on HOMER toolbox¹⁸.

In both fMRI and NIRS data, the low-frequency fluctuations were obtained by band-pass filtering the data in the region between 0.008 and 0.09 Hz.

2.3. Graph construction and analysis

We computed graphs independently for each hemodynamic signal (BOLD or hemoglobin concentration). For a given signal, we defined each ROI (fMRI) or channel (NIRS) as a node. The link between two nodes was based on the Pearson correlation coefficient, ρ , between the times series. We set a threshold for ρ , so that for $\rho \geq$ threshold we established a link between two nodes. Otherwise, there was no link. Since the threshold introduces a degree of freedom in the analysis, we varied the threshold from 0.05 to 0.75.

We then computed global graph parameters for each run of each subject as function of the correlation threshold. We analyzed the total number of links of the graph (N), the average degree (K), the distribution of the degree of the nodes by measuring the standard deviation of the degree (StdK), and the clustering coefficient (CC) of the graph²⁰⁻²².

In order to analyze group results, we decided not to employ averages but rather to compute frequency of appearance. Therefore, our approach allows us to analyze common features between subjects, rather than analyzing average behavior that might not reflect any specific subject. To extract a graph that carried robust features of each subject, we fixed the number of links of each graph as 20% of the maximum possible number of links. With this approach, we created binary graphs by keeping only the strongest connections of each run as measured by the Pearson correlation coefficient. In addition, by proceeding with this method, we could account for both the different number of nodes of each network and the variability in the potential physiological contamination of the signal from each subject. (Note, subjects who were more contaminated by physiological noise naturally present connections with higher correlation values. We have discussed this approach on previous works^{3,8}). Once we had one graph for each run, we combined all graphs of all runs from the same subject, and kept only the links that were presented in at least 50% percent of the runs of each subject. We last combined resultant graphs of all subjects to create a frequency network, which carries the frequency that each connection appeared over the subjects.

3. Results and Discussion

As an illustration, Figure 1 shows resultant graphs for two representative subjects obtained with HbO₂ data from NIRS when the threshold for ρ

was set at 0.5. We obtained similar graphs for other thresholds and hemodynamic signals. By visually comparing the two NIRS-based graphs in Figure 1, one can clearly see that the graphs between the two subjects are very different, although there are few similar links. From one end, a degree of similarity is expected since the human brain is a result of evolution and works through the development of structure and function. On the other hand, the result presented in Figure 1 is somewhat expected since there is no reason to expect that the brain from two different persons would function similarly during the experiment.

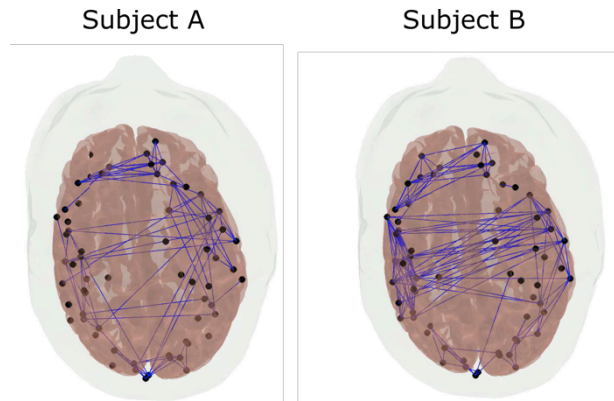


Figure 1. Top view of resultant graphs for two representative subjects using the HbO₂ signal and $\rho=0.5$. The black dots represent the nodes (in this case, NIRS channels) and the blue lines represent the links (in this case, channels with $\rho \geq 0.5$).

Despite the difference in the connections of the two graphs, their global parameters are strikingly similar. The average degree of the graphs from subjects A and B in Figure 1 are both 0.13, with a spread (i.e., standard deviation) of 0.07 and 0.09, respectively. The clustering coefficient for subject A in Figure 1 is 0.53; for subject B this parameter is 0.58. This result suggests that, despite connections may vary across different subjects, and even for the same subject at different periods of time, the type of graph for the human brain at rest may have similar properties.

The similarity of the graph parameters for all subjects in our cohort becomes evident in the small error bars of Figure 2, which represent the standard error of each graph parameter across all subjects, for all hemodynamic signals and different correlation thresholds.

To quantify the variability across subjects, we calculated the ratio between the standard error and the mean value of each parameter for each correlation threshold. We observed that the mean variations across subjects for the average degree were on the order of 15% for all hemodynamic signals. The variability of the clustering coefficient is even smaller, reaching no more than 7%.

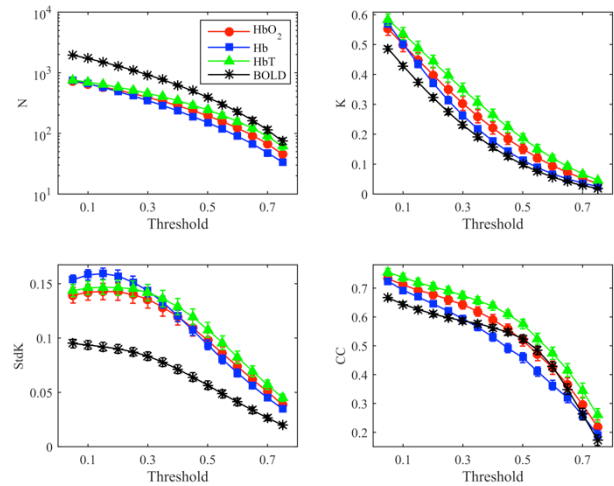


Figure 2. Variation of the graph parameters across all 20 subjects for all hemodynamic signals and thresholds used. The parameters computed were the total number of links (N), the average degree (K), the standard deviation of the degree distribution (StdK) and the clustering coefficient (CC). Oxy- (HbO₂, red), deoxy- (Hb, blue) and total-hemoglobin (HbT, green) concentrations come from NIRS, while the BOLD signal (black) comes from fMRI. The error bars represent the standard error across all subjects.

Regarding the dynamics of the graph metrics as function of the order parameter, Figure 2 shows that the graph parameters decay as the correlation threshold increases. This behavior is expected since an increase in the threshold means that lesser connections would be available. In addition, the distribution of the number of links for each node tends to increase for low thresholds, reaching its maximum at approximately 0.25. This result reflects that the high density of connections for the graphs built up to this threshold is probably due to spurious noise in the data.

Last, we attempted to quantify common patterns in the graphs for the whole group. Figure 3 shows frequency graphs that were created based on the frequency of appearance of each link across all the subjects for each of the hemodynamic signals. This approach allows investigation of the connectivity links that are present in almost all subjects. In this study, we observed that despite high variability of the links across subjects (Figure 1), a total of 54, 41, 50 and 301 links were consistently present in at least 75% of all subjects when we considered, respectively, HbO₂, Hb, HbT and BOLD frequency graphs. (Note, the higher number of nodes (90) in the BOLD graph is one of the reasons for the higher number of links in this graph.)

Concerning location, the most frequent links are consistently observed in the frontal-parietal region, which can be related to superior tasks. By analyzing individual graphs for each subject, it is possible to note that other brain regions exhibit a high density of links, particularly between regions that are symmetrically located or among areas that share the same functionality. However, most of these connections are subject-specific and did not achieve significant frequency. The relatively low number of common connections reinforces the fact that the variability across subjects should be neglected.

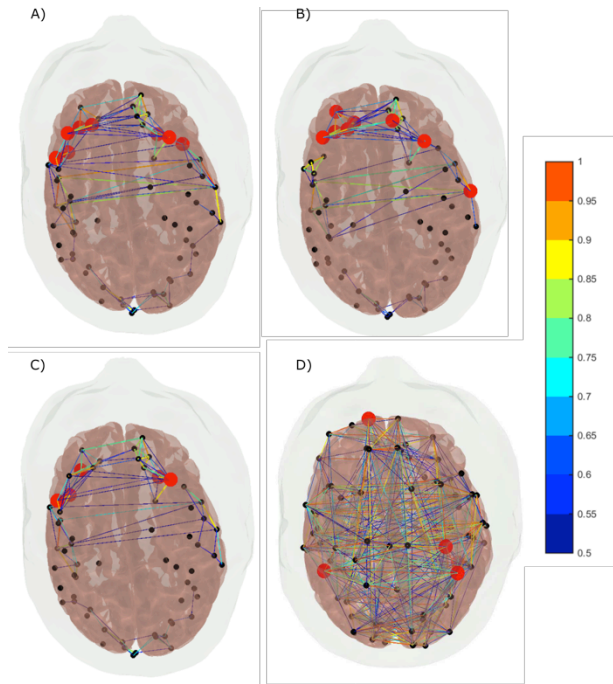


Figure 3. Frequency graphs for (A) oxy-hemoglobin, (B) deoxy-hemoglobin, (C) total-hemoglobin and (D) BOLD-fMRI. The black dots represent the nodes of the graph, while the red dots are the hubs (i.e., most connected nodes). The links are color-coded by their frequency of appearance across all 20 subjects.

Among several cortical regions measured, few of them were highly connected to other regions (i.e., they were hubs in the graph). These regions were identified as red dots in Figure 3. Overall, we found 8, 8, 5, and 4 regions in the HbO₂, Hb, HbT and BOLD graphs. Most of the nodes were located in the frontal lobe, with slightly predominance from the left hemisphere. We previously found a similar left hemisphere predominance for another NIRS data cohort, and this asymmetrically result has been previously reported in the literature¹⁴.

Although the above-cited results are very encouraging, it is important to highlight their limitations regarding its interpretation. First, NIRS and fMRI have different time-series properties despite its common hemodynamic origin. fMRI temporal acquisition is slow (~ 2 s) which leads to aliasing from global, systemic physiology that cannot be removed from data²³. On the other hand, NIRS high temporal resolution (~ 100 ms) provides autocorrelated time-series over several data points, which can lead to spurious high Pearson correlation coefficients²⁴. Concerning its biological interpretation, it is important to remind that the hemodynamic changes measured by either fMRI or NIRS may not be directly related to neural changes. Although several studies show an unquestionable correlation between neural changes and NIRS/fMRI signals, the relationship underlying neurovascular coupling as well as its relationship to each observable are still not fully understood. Therefore, the connection and interpretation between results derived from either NIRS or fMRI, as well as their comparison, must

take into account the different and inherent properties of each technique.

4. Conclusions

In this work we aimed to better understand the spatial-temporal interactions of brain function at rest by using graph theory in multimodal neuroimaging data. We simultaneously employed NIRS and BOLD-fMRI in 20 healthy, young subjects. Unlike the majority of the previous studies, we attempted to characterize the individual resting state graphs. We could observe that, despite different subjects have different connectivity patterns, the characteristic of their graphs (as measured by its global graph properties) are surprisingly similar as pointed by the small population variances. The inter-subject variability ranged from 10% to 15%, depending on the parameter analyzed. This result suggests that the resting state connectivity maps can be thought of different microstates associated to one single macrostate defined by its properties. On the other hand, the different connectivity patterns for each subject led us to think about common characteristics across subjects. In order to appropriately address this scientific question, we derived a novel graph based on frequency distribution of links. We strongly believe that the analysis and further validation of frequency graphs can lead to significant contributions regarding common characteristics of groups of subjects, but at the same time will allow us to better understand functional brain individualization.

Acknowledgments

The authors thank M. Cordeiro for help with the MRI acquisition, and Carlos Stefano and Gabriela Castellano for helpful discussions. This work was supported by the São Paulo Research Foundation (FAPESP) through 2012/02500-8 and 2013/07559-3. Additional support was obtained by CNPq and CAPES.

References

1. Raro, S. M., Bandettini, P. A., Binder, J. R., Bobholz, J. A., Hammeke, T. A., Stein, E. A., Hyde JS. Relationship Between Finger Movement Rate and Functional Magnetic Resonance Signal Change in Human Primary Motor Cortex. *J Cereb Blood Flow Metab.* 1996;16(6):1250-1254.
2. C. S. Roy, Sherrindton CS. On the regulation of the blood-supply of the brain. *J Physiol.* 1890;11.
3. Forero, Edwin J., Novi, Sergio L., Avelar, Wagner m., Anjos, Carlos A., Menko, Julien G., Forti, Rodrigo M., Oliveira, Vinicius R., Cendes, Fernando, Covolan, Roberto J. M., Mesquita RC. Use of near-infrared spectroscopy to probe occlusion severity in patients diagnosed with carotid atherosclerotic disease Abstract : *Med Res Arch.* 2017;5(6):1-22.
4. Strangman G, Culver JP, Thompson JH, Boas DA. A quantitative comparison of simultaneous BOLD fMRI and NIRS recordings during functional brain activation. *Neuroimage.* 2002;17(2):719-731. doi:10.1016/S1053-8119(02)91227-9.
5. Heekeren HR, Obrig H, Wenzel R, et al. Cerebral haemoglobin oxygenation during sustained visual stimulation - a near-infrared spectroscopy study. *Philos Trans R Soc B Biol Sci.* 1997;352(1354):743-750. doi:10.1098/rstb.1997.0057.

6. Attwell D, Laughlin SB. An Energy Budget for Signaling in the Grey Matter of the Brain. *J Cereb Blood Flow Metab.* 2001;1133-1145. doi:10.1097/00004647-200110000-00001.
7. Bullmore ET, Sporns O. Complex brain networks: graph theoretical analysis of structural and functional systems. *Nat Rev Neurosci.* 2009;10(3):186-198. doi:10.1038/nrn2575.
8. Novi SL, Rodrigues RBML, Mesquita RC. Resting state connectivity patterns with near-infrared spectroscopy data of the whole head. *Biomed Opt Express.* 2016;7(7):2524-2537. doi:10.1364/BOE.7.002524.
9. Mesquita RC, Franceschini MA, Boas DA. Resting state functional connectivity of the whole head with near infrared spectroscopy. *Biomed Opt Express.* 2010:324-336. doi:10.1364/BOE.1.000324.
10. Biswal BB, Yetkin FZ, Haughton VM, Hyde JS. Functional connectivity in the motor cortex of resting human brain using echo-planar MRI. *Magn Reson Med.* 1995;34(4):537-541. doi:10.1002/mrm.1910340409.
11. Sanz-Arjiga EJ, Schoonheim MM, Damoiseaux JS, et al. Loss of "Small-World" Networks in Alzheimer's Disease: Graph Analysis of fMRI Resting-State Functional Connectivity. *PLoS One.* 2010;5(11). doi:10.1371/journal.pone.0013788.
12. Garrity AG, Pearlson GD, McKiernan K, Lloyd D, Kiehl KA, Calhoun VD. Aberrant "default mode" functional connectivity in schizophrenia. *Am J Psychiatry.* 2007;164(3):450-457. doi:10.1176/appi.ajp.164.3.450.
13. Safonova LP, Michalos A, Wolf U, et al. Age-related changes in cerebral hemodynamics assessed by near-infrared spectroscopy. *Arch Gerontol Geriatr.* 2004;39(3):207-225. doi:10.1016/j.archger.2004.03.007.
14. Yasuda CL, Chen Z, Beltramini GC, et al. Aberrant topological patterns of brain structural network in temporal lobe epilepsy. *Epilepsia.* 2015;56(12):1992-2002. doi:10.1111/epi.13225.
15. Power JD, Mitra A, Laumann TO, Snyder AZ, Schlaggar BL, Petersen SE. Methods to detect, characterize, and remove motion artifact in resting state fMRI. *Neuroimage.* 2014;84:320-341. doi:10.1016/j.neuroimage.2013.08.048.
16. Landeau B, Papathanassiou D, Crivello F, et al. Automated Anatomical Labeling of Activations in SPM Using a Macroscopic Anatomical Parcellation of the MNI MRI Single-Subject Brain. 2002;15:273-289. doi:10.1006/nimg.2001.0978.
17. Campos BM De, Coan AC, Yasuda CL, Casseb RF, Cendes F. Large-Scale Brain Networks Are Distinctly Affected in Right and Left Mesial Temporal Lobe Epilepsy. 2016;3152(May):3137-3152. doi:10.1002/hbm.23231.
18. Huppert TJ, Diamond SG, Franceschini MA, Boas DA. HomER: a review of time-series analysis methods for near-infrared spectroscopy of the brain. *Appl Opt.* 2009;48(10):280-298. doi:10.1016/j.drugalcdep.2008.02.002.A.
19. Carbonell F, Bellec P, Shmuel A. Global and system-specific resting-state fMRI fluctuations are uncorrelated: principal component analysis reveals anti-correlated networks. *Brain Connect.* 2011;1(6):496-510. doi:10.1089/brain.2011.0065.
20. Rubinov M, Sporns O. Complex network measures of brain connectivity: Uses and interpretations. *Neuroimage.* 2010;52(3):1059-1069. doi:10.1016/j.neuroimage.2009.10.003.
21. van den Heuvel MP, Hulshoff Pol HE. Exploring the brain network: A review on resting-state fMRI functional connectivity. *Eur Neuropsychopharmacol.* 2010;20(8):519-534. doi:10.1016/j.euroneuro.2010.03.008.
22. Fornito A, Zalesky A, Bullmore ET. *Fundamentals of Brain Network Analysis.* Elsevier; 2016.
23. Fox MD, Raichle ME. Spontaneous fluctuations in brain activity observed with functional magnetic resonance imaging. *Nat Rev Neurosci.* 2007;8(9):700-711. doi:10.138/nrn2201.
24. Santosa H, Perlman SB, Huppert TJ, et al. Characterization and correction of the false-discovery rates in resting state connectivity using functional near-infrared spectroscopy. 2017;22(5). doi:10.1117/1.JBO.22.5.055002.

Contato:

Sergio Luiz Novi Junior
 Universidade Estadual de Campinas
 e-mail: novisl@ifi.unicamp.br